

STEP SKEWING ROTOR DESIGN OF PERMANENT MAGNET BLDC MOTOR FOR INWHEEL ELECTRIC VEHICLE

THIẾT KẾ ĐỘNG CƠ MỘT CHIỀU KHÔNG CHỐI THAN NAM CHÂM VĨNH CỬU RÃNH NGHIÊNG CHO BÁNH XE ĐIỆN

Bui Minh Dinh^{1,*}, Nguyen Viet Anh²

ABSTRACT

Permanent magnetic brushless direct current motor (PM BLDC) can be designed with different rotor configurations based on the arrangement of the permanent magnets. Rotor configurations strongly influence the torque an efficiency performance of permanent magnet electrical motors. Most of the applications prefer surface mounted permanent magnet design due to its ease of construction and maintenance in [1]. The aim of this paper is to compare and evaluate different rotor configurations for PM BLDC motor with or without skewed stator slot. A finite element method has been used for analysis and comparison of different geometry parameters and configurations in [2-4]. This paper describes a comprehensive design of a three phase PM BLDC motor 20kW for in wheel. An optimal design of PMBLDC motor have been implemented by analytical and simulation methods.

In this paper, the skewing slot is applied to the PM surface mounted Brushless DC Motor 20kW 36 slots and 12 magnet poles ($Z = 36, p = 12$) for eliminating torque ripples. To observe the skewing stator effect, the stator lamination layers are skewed with different angles. With determined skewing angle, the cogging torque eliminated theoretically and flux density space harmonics are also reduced.

Keywords: Permanent Magnetic Brushless Direct Current Motor, Finite Element Method, Ansys Maxwell, SPEED software, Magnetic flux density.

TÓM TẮT

Động cơ một chiều không chổi than nam châm vĩnh cửu (PM BLDC) có thể được thiết kế với hình dạng rôto khác nhau dựa trên sự sắp xếp của các nam châm vĩnh cửu. Do cấu hình rôto có ảnh hưởng mạnh mẽ đến hiệu suất mô men điện từ trong động cơ nam châm vĩnh cửu. Nên hầu hết các ứng dụng đều thiết kế nam châm vĩnh cửu gắn trên bề mặt do dễ dàng trong chế tạo và bảo trì [1]. Nghiên cứu này có mục đích so sánh và đánh giá cấu hình rôto khác nhau cho động cơ PM BLDC có hoặc không có rãnh lệch ở stato. Phương pháp phần tử hữu hạn được sử dụng để phân tích và so sánh các thông số và hình dạng rôto khác nhau [2, 4]. Bài báo mô tả thiết kế toàn diện động cơ ba pha PM BLDC 20kW cho bánh xe điện. Thiết kế tối ưu được thực hiện bằng phương pháp phân tích và mô phỏng.

Trong bài báo này, rãnh nghiêng được áp dụng cho nam châm gắn bề mặt động cơ một chiều không chổi than 20kW, 36 rãnh và 12 cực nam châm ($Z = 36, p = 12$) để loại bỏ gợn sóng mô men điện từ. Khi quan sát hiệu ứng lệch rãnh stato, các lớp thép stato bị lệch ở các góc khác nhau. Với một góc lệch xác định, gợn sóng mô men bị loại bỏ về mặt lý thuyết và sóng hài không gian do mật độ từ thông sinh ra được giảm xuống.

Từ khóa: Động cơ một chiều không than nam châm vĩnh cửu, phương pháp phần tử hữu hạn, Ansys Maxwell, phần mềm SPEED, mật độ từ thông.

¹Faculty of Electrical Engineering, Hanoi University of Science and Technology

²Faculty of Electrical Engineering, Hanoi University of Industry

*Email: dinh.buiminh@hust.edu.vn

Received: 20/7/2021

Revised: 15/10/2021

Accepted: 15/11/2021

1. INTRODUCTION

Permanent magnetic brushless direct current motor (PM BLDC) have been widely used because of their attractive features like compactness, low weight, high efficiency, and ease in control [1]. The reliability of PM BLDC motor is high since it does not have any brushless to wear out and replace. The stator consists of stacked steel laminations with windings placed in the slots where as the rotor is made of permanent magnet that can vary from two to twelve pole pairs with alternate north and south poles.

A large number of PM BLDC applications require minimized torque ripple for reduced vibration and acoustic noise, and smooth operation of the motor. In addition, low torque pulsations in motor drives are essential for high-performance speed and position control applications where friendly human-machine interactions are desired. The three main components of torque in PM BLDC are asfollows:

- 1) Mutual torque, which is caused by the interaction of the rotor field and stator currents;
- 2) Reluctance torque, which is due to the rotor saliency;
- 3) Cogging torque, which arises from the interaction between permanent magnets (PMs) and slotted iron structure.

The contribution from reluctance torque in surface-mounted PM BLDCs, also known as surface PM (SPM) machines, can be ignored since the difference between the direct-and quadrature-axis reactances is negligible.

The output torque quality can be improved by reducing the torque ripple in the mutual torque, which is related to the harmonics in the back-EMF (BEMF). Reducing the cogging torque will also improve the output torque quality. Methods for reducing cogging torque and for minimizing the BEMF harmonic contents to minimize the torque ripple appear in [5-12]. Some researchers have addressed the torque ripple problem in PM BLDCs primarily from a design point of view [6-8], while others worked from the control side [10, 11]. Several researchers have shown that the improvement in cogging torque leads to the improvement in torque ripple [8]. One of the well-known approaches to minimize cogging torque is rotor or stator skewing. Cogging or detent torque in PM BLDCs can be theoretically reduced to zero by the selection of optimum skew angle, which can be achieved through a suitable choice of slot-pole combination [10].

This paper presents a detailed analysis of torque ripple variation under field-weakening operation and also cogging torque variation with different magnet shapes and skewing. This paper shows that the torque ripple can either decrease or increase after magnet skewing when step-skew techniques are used. Step skewing is a common practice in the industry adopted for ease of manufacturing and cost reductio. FEM has been applied to design BLDC motor widely in [15].

2. PM BLDC MOTOR DESIGN AND ANALYSIS

The analysis is being carried out for a three phase BLDC motor. Magnet Vacodym 677 HR is magnet material used due to its good thermal stability allowing its use in applications exposed to high temperature about 180°C. The flux density is selected about 0.8T.

$$\mu_0 \mu_m = \frac{\Delta H}{\Delta B} \rightarrow \mu_m = \frac{\Delta H}{\mu_0 \Delta B} = \frac{1.18T}{915kA / m \mu_0} = 1.026 \quad (1)$$

The geometry specifications of the motor used for the analysis are listed in Table 1.

Table 1. Geometry parameters of PMLDC Motor

No	Parameters	Unit
1	Outer diameter	218mm
2	Rotor diameter	116mm
3	Slot length	112mm
4	Normal Torque	200Nm
5	Maximum Torque	350Nm
6	Speed	3600rpm
7	Slot Number	18
8	Power	20kW
9	Stator Bore	142
10	Tooth Width	7mm
11	Slot Depth	29mm
12	Pole Number	12
13	Magnet Thickness	4mm
14	Number turn per coil	12

The design requirements are low cost, overload capacity, complex controller, efficiency and reliability. For

electric vehicle applications, the manufacturing cost, complex controller are not so important, but efficiency is the first priority of this design. With those requirements above, a layout of BLDC motor was calculated by SPEED software shown in Figure 1.

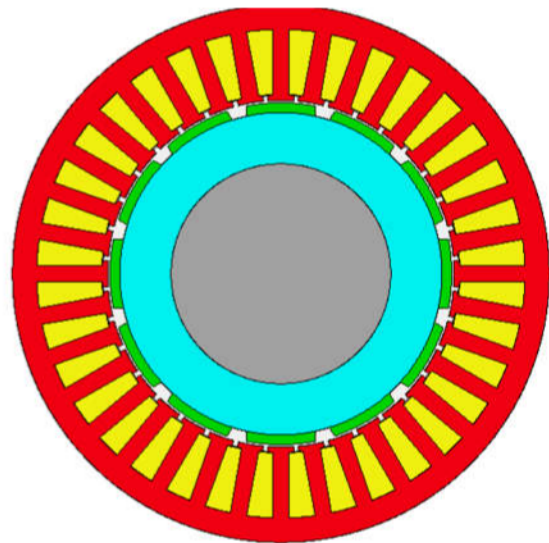


Figure 1. Layout of a BLDC Motor Z = 36, p = 12

Based on this design, some basic performances are shown in Figure 2. The most important parameter is efficiency of 95.2% which is target of the proposal design in full efficiency map in figure 5. In order to obtain maximum efficiency value, the BLDC motor is optimized by control angles from 0 to 360/2p = 12 degree. The torque on the shaft is 180 Nm with 200VDC and current of 180 A.

Table 2. Torque and efficiency results of PMLDC Motor Z = 36, p = 12

Parameter	Value	Unit
Average torque (virtual work)	180.21	Nm
Average torque (loop torque)	179.07	Nm
Torque Ripple (MsVw)	14.74	Nm
Torque Ripple (MsVw) [%]	8.17	%
Cogging Torque Ripple (Ce)	13.92	Nm
Cogging Torque Ripple (Vw)	14.26	Nm
Speed limit for constant torque	918.39	rpm
Electromagnetic Power	18884	Watts
Input Power	20632	Watts
Output Power	18679	Watts
Total Losses (on load)	1953.33	Watts
System Efficiency	90.53	%
Shaft Torque	158.37	Nm

In order to evaluate the maximum torque of the motor, a maximum current is applied to determine torque is 178Nm at speed of 3600rpm with a current I = 200A and the efficiency is quite low about 90.53%. However, this design is still not yet optimal. To improve the design, different motor configurations, controlling angles can be adjusted to achieve maximum efficiency but the geometry parameters in Table 1 are kept constant.

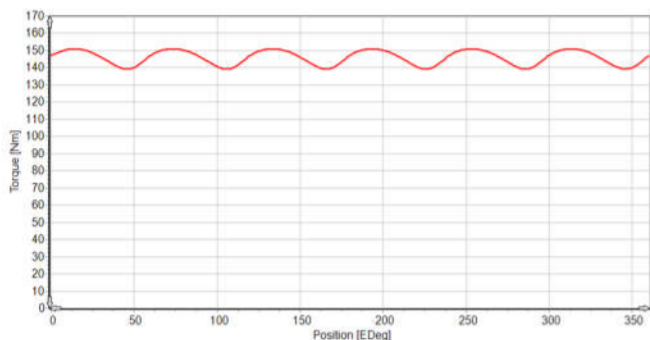


Figure 2. Average torque of a BLDC Motor Z = 36, p = 12

Based on this simulation, the electromagnetic torque curves have also determined at different rotor positions from 0 to 360 and I = 200A as Figure 2.

A 2D BLDC motor model is simulated by FEMM software. After meshing the geometry model included magnetic NdFe42, silicon steel M27 or 35A470 and insulation materials, the electromagnetic characteristics have been obtained and the flux density distribution of rotor and stator is resulted at 3600rpm and 200A in figure 3.

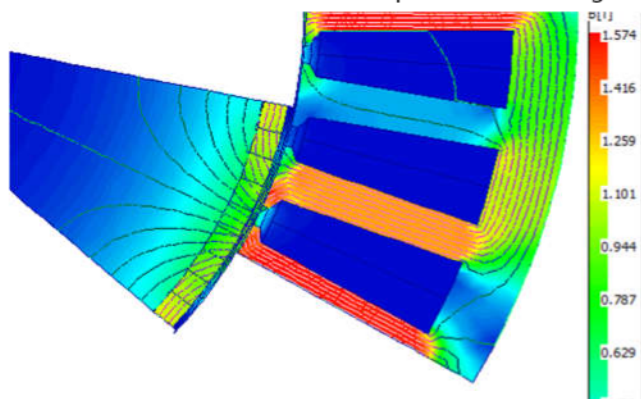


Figure 3. Flux density results

Back EFM has been investigated at different modes such as no-load, full load at different speed. Many steps of rotor position and currents, the torque and flux density results have recorded and saved in Matlab files to plot those characteristics. Electromagnetic forces were calculated at different speeds in Figure 4. The electromagnetic forces can be obtained by analytical method as equations:

$$e = -\frac{d\psi}{dt} = -\frac{d\psi}{d\theta} \cdot \frac{d\theta}{dt} = -\frac{d\psi}{d\theta} \cdot 2\pi \cdot n \approx -\frac{\Delta\psi}{\Delta\theta} \cdot 2\pi \cdot n \quad (2)$$

For overall torque vs speed curves under normal and overload capacity, a full efficiency map was plotted with 200 VDC/300 A and maximum current density of 15A/mm². There are many efficiency curves however efficiency level from 90% to 96% in below figure can cover or meet requirement of the BLDC Motor 20kW - 3600rpm.

It ensures that the motor cooling system can't not exceeded limit temperatures of winding (160°C) and magnet (140°C). Peak torque of 300Nm is constant with speed to 1200rpm and to down from 1200 to 10000rpm. With normal torque of 150Nm, the constant speed is

extended to 2000rpm and maximum speed of 10000rpm the average torque is 30Nm.

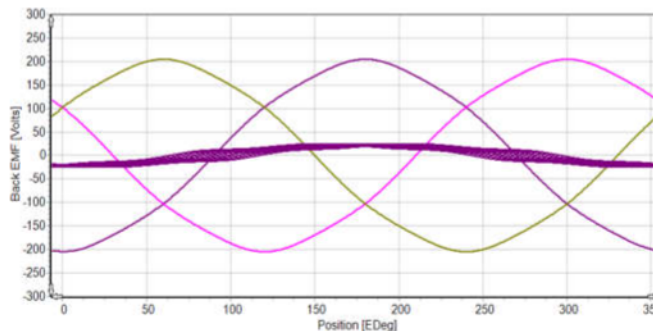


Figure 4. Back EMF results

3. SKEW ANGLE CALCULATION

Skewing method is used frequently in BLDC motors for eliminating this cogging torque. With optimum skew angle, cogging torque can be eliminated theoretically. Skewed rotor for the stator lamination layers are illustrated in Figure 5.

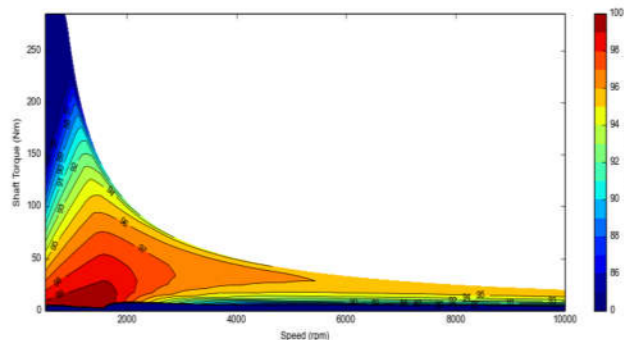


Figure 5. Full efficiency map

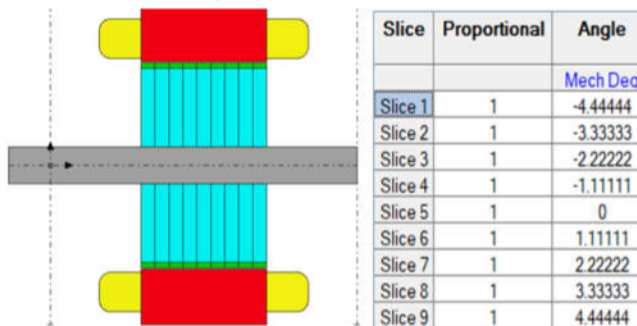


Figure 6. 9 Slice step-skewing rotor

Any consecutive slices are numbered as 1 and 2 in Figure 6 to show the beginning position for the first slice to last slice. Depending on optimum skew angle, each slice should be skewed one by one by skewing angle and number slices.

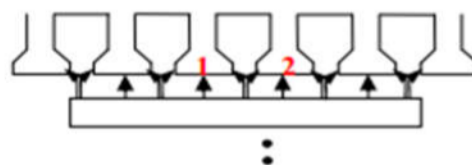


Figure 7. Cogging torque analysis of slice skewing

Cogging torque can be calculated from stored energy in the air gap. Variation of the co-energy gives the cogging torque [13].

$$T_c = \frac{dW}{d\theta} \tag{3}$$

Where T_c is the cogging torque, $\partial\theta$ is the displacement with mechanical degree, ∂W is the stored co-energy in the air gap.

Cogging torque is periodic along the air gap. By using this periodicity feature, Fourier series of the cogging torque can be obtained [14].

$$T_{skew}(\theta) = \sum_{i=1}^{\infty} K_{sk} \cdot T_i \cdot \sin(iC_p \theta_m + \theta_i) \tag{4}$$

Where K_{sk} is the skew factor which is 1 for non-skewed motor laminations. C_p is least common multiple between the number of pole and number of stator slots, T_i is absolute values of the harmonics, θ_m is the mechanical angle between stator and rotor axis while motor is rotating and represent to the phase angle K_{sk} , that is skew factor, the defined by:

$$K_{sk} = \frac{\sin\left(\frac{iC_p \alpha_{sk}}{N_s}\right)}{\frac{iC_p \alpha_{sk}}{N_s}} \tag{5}$$

Where α_{sk} is the skew angle and N_s is the number of slices. Skew angle is given in Equation (6).

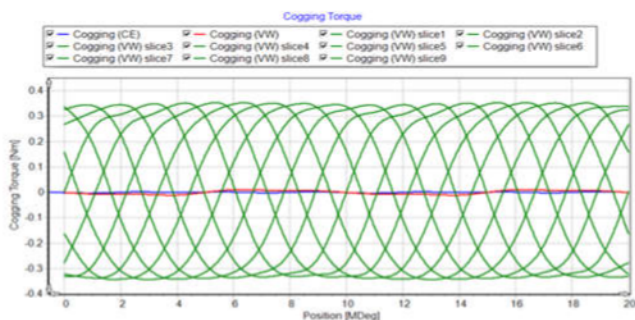


Figure 8. Cogging torque of 9 slices and reduced cogging torque

Average values of load torques are nearly same values for even one slot pitch skewed motor result in terms of average load torque are coherent with the non-skewed motor model. To relative torque ripples can be calculated as follows:

$$T_{ripple} = \frac{(T_{max} - T_{min})}{T_{avg}} \tag{6}$$

If increasing skew angle, the torque ripple is reducing but the average torque will be down also but the manufacturing and assembly technologies are big challenges.

4. CONCLUSION

The paper has presented a comprehensive design of a PMLBDC motor 20kW - z = 36, p = 12 for in wheel electric vehicles. The design was calculated by analytical method, optimized by SPEED software and evaluated electromagnetic characteristics by FEM. Particularly, detail results of torque, efficiency was compared and analyzed under different

operation. The step skewing slice rotor is applied to the PM surface mounted type Brushless DC Motor for eliminating torque ripples. To observe the skewing effect, the rotor magnet segment (or slices) are skewed with different angles. The best skewing angle is determined by number of slices and skewing angle with a parametrical study.

REFERENCES

[1]. Sandeep Kumar Chawrasia, Aakash Das, Chandan Kumar Chanda, 2020. *Design and Analysis of Electric bike Hub-Motor using Motor-CAD*. 2020 3rd International Conference on Energy, Power and Environment: Towards Clean Energy Technologies.

[2]. Chunhua Liu, K. T. Chau, J. Z. Jiang, 2008. *A Permanent-magnet Hybrid In-wheel Motor Drive for Electric Vehicles*. IEEE Vehicle Power and Propulsion Conference (VPPC), Harbin, China, September 3-5.

[3]. S. Tatipamula, 2013. *Study of Parallel Electric Hybrid Three-Wheeled Motor Taxi*. International Journal of Computer Applications (0975-8887), pp. 38-39.

[4]. B. Tabbache, S. Djebbari, A. Kheloui, Md. Benbouzid, 2013. *A Power Presizing Methodology for Electric Vehicle Traction Motor*. International Review on Modelling and Simulations.

[5]. P.Pillay, R.Krishnan, 1989. *Modeling, Simulation and Analysis of Permanent-Magnet Motor Drives, Part II: The Brushless DC Motor Drive*. IEEE Trans. on Industry Applications, pp.274-279.

[6]. V. Petrovic, R. Ortega, A. M. Stankovic, G. Tadmor, 2000. *Design and implementation of an adaptive controller for torque ripple minimization in PM synchronous motors*. IEEE Trans. Power Electron., vol. 15, no. 5, pp. 871-880.

[7]. S. M. Hwang, J. B. Eom, Y. H. Jung, 2001. *Various design techniques to reduce cogging torque by controlling energy variation in permanent magnet motors*. IEEE Trans. Magn., vol. 37, no. 4, pp.2806-2809.

[8]. N. Bianchi, S. Bolognani, 2002. *Design techniques for reducing the cogging torque in surface-mounted PM motors*. IEEE Trans. Ind. Appl., vol. 38, no. 5, pp. 1259-1265.

[9]. P. Ji, W. Song, Y. Yang, 2003. *Overview on application of permanent magnet brushless DC motor*. Electrical Machinery Technology, vol.40, pp.32-36.

[10]. M. Dai, A. Keyhani, T. Sebastian, 2004. *Torque ripple analysis of a PM brushless DC motor using finite element method*. IEEE Trans. Energy Convers., vol. 19, no. 1, pp. 40-45.

[11]. F. Libert, J. Soulard, 2004. *Design study of different Direct-Driven Permanent-Magnet Motors for a low Speed Application*. Nordic Workshop on Power and Industrial Electronics (NORpie), pp.1-6.

[12]. L. Dosiek, P. Pillay, 2006. *Cogging torque reduction in permanent magnet machines*. 41st IAS Annual Meeting vol.1, pp. 44-49.

[13]. A. Ahmed, D. D. Bhutia, 2015. *Propulsion System Design and Sizing of an Electric Vehicle*. International Journal of Electronics and Electrical Engineering, Volume 3, No. 1.

[14]. J.R. Hendershot, T.J.E. Miller. 1994. *Design of brushless Permanent magnet motors*. Magna Physics publishing and Clarendon press-Oxford.

[15]. Guangwei Meng, Hao Xiong, Huaishu Li, 2009. *FEM Analysis and simulation of Multi-phase BLDC Motor*. The 12th International Conference on Electrical Machines and Systems, ICEMS.

THÔNG TIN TÁC GIẢ

Bùi Minh Định¹, Nguyễn Việt Anh²

¹Viện Điện, Trường Đại học Bách khoa Hà Nội

²Khoa Điện, Trường Đại học Công nghiệp Hà Nội